A 2D Model for Bulk Acoustic Wave Devices using a Dyadic Green's Function of Laminar Plate

24th European Frequency and time Forum
13-16 April 2010

Sylvain Ballandras[(1)], William Daniau[(1)], Julien Garcia[(1)], Thierry Laroche[(1)], Alexandre Reinhardt[(2)]

[(1)]FEMTO-ST, CNRS-UFC-ENSMM-UTBM UMR 6174,
32 Avenue de l'Observatoire, 25044 Besançon Cedex, FRANCE
Email: sylvain.ballandras@femto-st.fr

[(1)]CEA-LETI, Laboratoire Composants Radio Fréquence
17 Rue des Martyrs, 38044 Grenoble Cedex, FRANCE
Email: alexandre.reinhardt@cea.fr

INTRODUCTION

Modern passive radio-frequency components devoted to telecommunication applications are exploiting thin overlays or membranes obtained along various approaches to benefit from acoustic modes with particular properties. For instance, Bulk Acoustic Waves (BAW) can be excited in thin Aluminum nitride or Zinc Oxide films, exhibiting strong piezoelectric coupling well suited for medium band filtering (relative bandwidth ranging from 2 to 5%). Although a lot of effort have been achieved to accurately simulate the behavior of such devices, promising approaches such as the developments proposed a few years ago based on dyadic Green's function of laminar plates [1] still received a small interest, contrarily to numerical methods using finite elements for instance which are massively used in that matter. However, it is still worth to have access to rapid and accurate models for design purpose, capable to integrate second order effects which finally actually contribute to device optimization. In the case of Surface Acoustic Waves (SAW), numerous achievements have been demonstrated in that matter [2], but for BAW, the alternative is either ultra-simple models or even equivalent circuits or massive numerical simulations.

The present work then is based on the above-mentioned Green's function. The main idea is to allow for the simulation of devices with finite width electrodes on the top side of the plate, the back side being grounded. We first neglect the influence of the electrode thickness but the approach is of course suited to account for such parameter. We particularly focus here on plates consisting of a single material, but this can be generalized to more complicated material stack. Along this approach, we are capable to accurately simulate actual devices with computation delays compatible with design purposes (a few minutes per configuration).

We first recall the calculation of these dyadic Green's function, presenting an alternative approach to the one already implemented [1] to ease their derivation. We then define an equivalent Green's function of the top surface and we analyze in details its physical properties. We show that the only singular contributions to this function are due to guided modes. Once subtracting these singularities, we then can propose an isomorphic description of this function, allowing to easily derive its inverse Fourier transform. We then propose a Chebychev development of the top boundary conditions to simulate bulk acoustic resonators. Comparison can be achieved with simpler models (for instance based on the Mason approach [3]) and finite element analysis [4] to emphasize the interest of this approach. Particularly, we discuss computation delays of the different approaches to point out the interest of the proposed one for design purposes as a conclusion.

DYADIC GREEN'S FUNCTION FOR LAMINAR PLATES

We assume the simple topology of an infinite laminar plate extending along the normal plate axis x_2 between –e and +e. Green's function for such a configuration has been first proposed by Reinhartd et al [1]. It is classically obtained by inverting the stress matrix and multiplying it with the displacement matrix, using the standard harmonic developments by

Fahmy-Adler or Christoffel as well [5]. Generalized normal stress $T.n$ and displacements u can be related to relative amplitudes A of partial waves composing the acoustic propagation as follows

$$\begin{Bmatrix} u(+e) \\ T.n(+e) \end{Bmatrix} = -j\omega \begin{bmatrix} [u_+^0] & [u_-^0] \\ [T_+^0] & [T_-^0] \end{bmatrix} \begin{bmatrix} [\Delta_+(+e)] & [0] \\ [0] & [\Delta_-(+e)] \end{bmatrix} \begin{Bmatrix} \{A_+\} \\ \{A_-\} \end{Bmatrix}$$
$$\begin{Bmatrix} u(-e) \\ T.n(-e) \end{Bmatrix} = -j\omega \begin{bmatrix} [u_+^0] & [u_-^0] \\ [T_+^0] & [T_-^0] \end{bmatrix} \begin{bmatrix} [\Delta_+(-e)] & [0] \\ [0] & [\Delta_-(-e)] \end{bmatrix} \begin{Bmatrix} \{A_+\} \\ \{A_-\} \end{Bmatrix} \quad (1)$$

where $\Delta(\pm e)$ is a matrix representing the wave distribution along x_2, upper-script 0 holds for eigenvalues and +/– index indicate incident and reflected waves. One can then form a comprehensive acoustic relation between both plate surfaces and then generalize somehow a Mason expression for the whole acoustic field. In that matter, one can write

$$\begin{Bmatrix} u(+e) \\ T.n(+e) \end{Bmatrix} = \begin{bmatrix} [u_+^0] & [u_-^0] \\ [T_+^0] & [T_-^0] \end{bmatrix} \begin{bmatrix} [\Delta_+(2e)] & [0] \\ [0] & [\Delta_-(2e)] \end{bmatrix} \begin{bmatrix} [u_+^0] & [u_-^0] \\ [T_+^0] & [T_-^0] \end{bmatrix}^{-1} \begin{Bmatrix} u(-e) \\ T.n(-e) \end{Bmatrix} \quad (2)$$

Consequently, one can use the standard matrix cascading methods developed for Mason and other matrix-based models [3, 5], but in our case displacements and stresses are vectors and not simply scalars, yielding more information concerning the acoustic distribution within the plate. These developments are very close to those proposed by Adler many years ago [6]. Once the cascade achieved, one can establish the laminar-plate Green's function as follows

$$\begin{Bmatrix} u(+e) \\ T.n(+e) \end{Bmatrix} = \begin{bmatrix} [A] & [B] \\ [C] & [D] \end{bmatrix} \begin{Bmatrix} u(-e) \\ T.n(-e) \end{Bmatrix} \Rightarrow \begin{Bmatrix} u(+e) \\ u(-e) \end{Bmatrix} = \begin{bmatrix} [A][C]^{-1} & [B]-[A][C]^{-1}[D] \\ [C]^{-1} & -[C]^{-1}[D] \end{bmatrix} \begin{Bmatrix} T.n(+e) \\ T.n(-e) \end{Bmatrix} \quad (3)$$

Along this approach, the laminar-plate Green's function is really simple to compute and is directly derived once the system (2) of any stacked material has been computed properly.

A NEW FORM OF THE PLATE GREEN'S FUNCTION ACCOUNTING FOR BOUNDARY CONDITIONS

We are now considering the case of a single material plate on which we intend to apply any surface excitation condition on the top surface, assuming the back side shorted electrically with an infinitely thin electrode. This particular boundary condition enables one to eliminate mechanical stress on this side but of course not the normal electrical displacement which must be accounted for respecting charge conservation. In a similar way, we neglect the mechanical stress on the top side induced by the presence of electrodes again assumed infinitely thin. Dissociating the electric and mechanical terms then yields the following expressions

$$\begin{Bmatrix} u_i(+e) \\ \varphi(+e) \\ u_i(-e) \\ 0 \end{Bmatrix} = \begin{bmatrix} \begin{bmatrix} G_{ij}^{tt} & G_{i4}^{tt} \\ G_{4j}^{tt} & G_{44}^{tt} \end{bmatrix} & \begin{bmatrix} G_{ij}^{td} & G_{i4}^{td} \\ G_{4j}^{td} & G_{44}^{td} \end{bmatrix} \\ \begin{bmatrix} G_{ij}^{dt} & G_{i4}^{dt} \\ G_{4j}^{dt} & G_{44}^{dt} \end{bmatrix} & \begin{bmatrix} G_{ij}^{dd} & G_{i4}^{dd} \\ G_{4j}^{dd} & G_{44}^{dd} \end{bmatrix} \end{bmatrix} \begin{Bmatrix} 0 \\ D_2(+e) \\ 0 \\ D_2(-e) \end{Bmatrix} \quad (4)$$

where the index only hold for sub-matrix developments, i and j varying from 1 to 3, upper-script d and t hold for down and top respectively. Setting the surface stress to zero enables one to establish a relation between normal electrical displacements on both surfaces, which naturally satisfies charge conservation and reads

$$D_2(+e) = -\frac{G_{44}^{dt}}{G_{44}^{dd}} D_2(-e) \quad (5)$$

Inserting this relation in (4) yields a scalar relation between the top surface potential and normal electrical displacement, yielding

$$\varphi(+e)=\left(G_{44}^{tt}-\frac{G_{44}^{dt}}{G_{44}^{dd}}G_{44}^{td}\right)D_2(+e) \tag{6}$$

Note that for a uniform 1Volt top surface excitation, one can easily derived the admittance given by

$$Y=j\omega\left(\frac{G_{44}^{dd}}{G_{44}^{tt}G_{44}^{dd}-G_{44}^{dt}G_{44}^{td}}\right)\Big|_{s_1=0} \tag{7}$$

in which the validity condition has been explicitly reported, i.e. the wave slowness along the surface s_1 must be zero as the excitation is not distributed upon surface. This provides the result reported in fig.1 which corresponds to the admittance of a planar resonator for a 50µm thick AT cut of quartz. The fundamental mode actually arises near 35 MHz (as expected) and only the odd harmonics are excited. At that point, we simply demonstrated the robustness of the proposed developments.

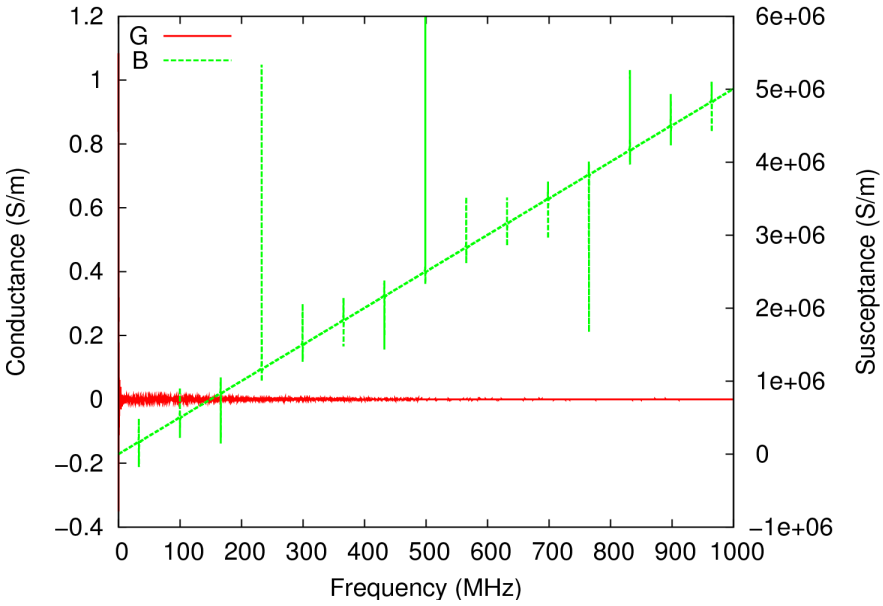

Fig.1 Electric admittance of a 50µm thick AT,X quartz cut with plane surfaces for an homogeneous surface excitation

REMARKABLE PROPERTIES OF THE NEW GREEN'S FUNCTION

We now observe the spectral properties of this new Green's function. Figure 2 shows its evolution along s_1, where one easily verifies its parity and purely imaginary nature [6] as no intrinsic losses are accounted for. One also can recognize the signature of guided modes as true poles modulating the slowly variating acoustic continuum. As the propagation of these modes is dispersive, they will depend on frequency. Furthermore, one can remark the finite value of the function near $s_1=0$ and its asymptotic behavior as $1/s_1$ for infinite slownesses. These features are fundamental as one expects to compute the inverse Fourier transform of this Green's function to allow for an actual representation of any electrode distribution atop the plate's surface. The finite value of the Green's function at zero slowness is modulated also by the frequency, as it increases dramatically near the bulk wave resonance.

The first analysis we propose here is to subtract the pole contributions as their form is pretty well known due to the numerous efforts developed in the frame of surface acoustic wave [7] modeling which reads

$$G(s_1) = Res + \left(\frac{G_p}{s_p - s_1} \right) \tag{8}$$

with G_p the amplitude of the pole (here purely imaginary) and s_p the pole slowness (purely real) and *Res* the residual contribution of the Green's function near the pole. These parameters are easily fitted using a 3-point algorithm proposed by Fusero et al, but this must be of course achieved for each frequency point of the analysis range. Figure 3 shows the efficiency of the pole subtraction for two given frequencies.

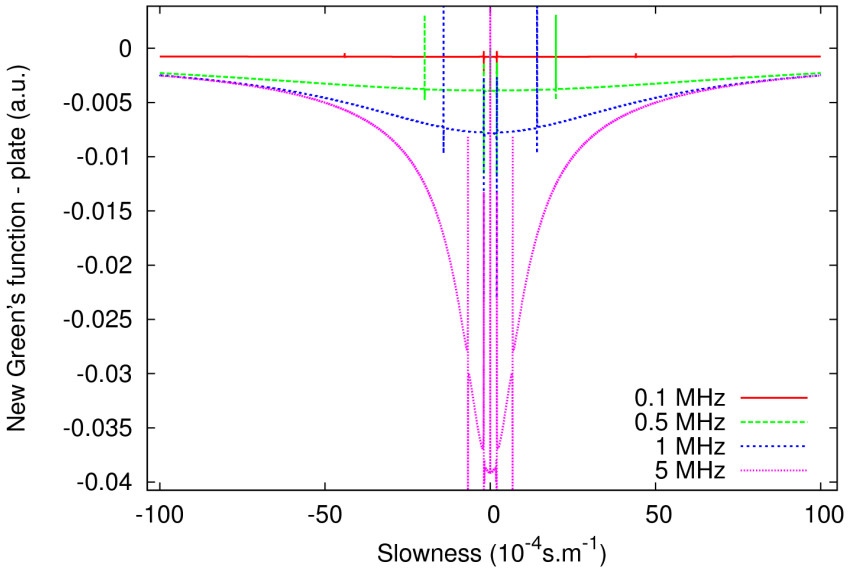

Fig.2 New Green's function versus slowness for a 50µm thick AT,X quartz cut for various frequencies

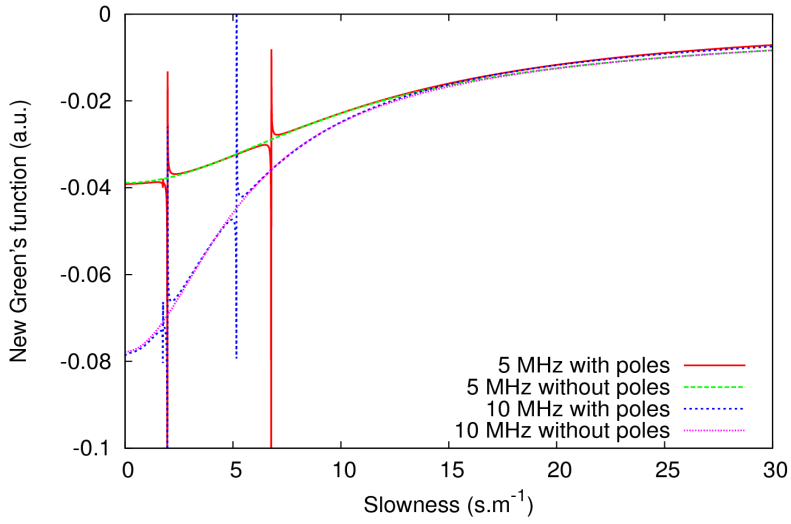

Fig.3 Suppression of the pole contributions for 2 given frequencies (slowness times 10^{-4})

Once suppressing the poles, one can see that the remaining function is holomorph, which means that its inverse Fourier transform can exist. We can consequently determine a rational function coinciding with this acoustic continuum and which

exhibits a known inverse Fourier transform. It turns out that the following function answers all the criteria with parameters that can be easily fitted using a non linear regression process

$$G_{Res}(\omega,s_1)=\frac{A_1(\omega)}{1+B_1(\omega)s_1^2}+\frac{A_2(\omega)}{1+B_2(\omega)s_1^2} \tag{9}$$

The implementation of the method shows that the residual continuum is well represented by the proposed model as illustrated in fig.4, with a residual error between the actual Green's function and the fitted one of less than 1% whatever the frequency is.

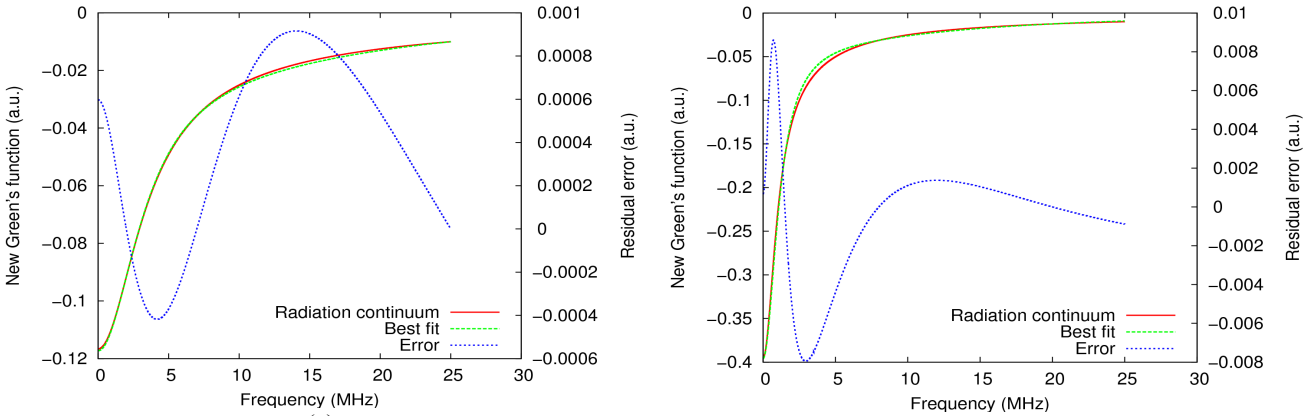

Fig.4 Comparison of the actual acoustic continuum of the new Green's function and its rational representation (9), calculation of the residual error at (a) 15 MHz et (b) 50 MHz (before and after the bulk resonance near 35 MHz)

SPATIAL GREEN'S FUNCTION

An important remark that must be reported here is that in all the presented developments, the angular frequency ω and the slowness s_1 are always dissociated. This characteristic is very useful for the computation of the inverse Fourier transform of our new spectral Green's function considering the following definition [6]

$$f(x_1)=\frac{1}{2\pi}\int_{-\infty}^{+\infty}F(k_1)e^{jk_1x_1}dk_1=\frac{\omega}{2\pi}\int_{-\infty}^{+\infty}F(\omega,s_1)e^{js_1\omega x_1}ds_1 \tag{10}$$

We can show that inverse Fourier transforms of the above-described contributions exist. Basing our investigations on [8,9] and considering that the reciprocal variable of s_1 is $\omega.x_1$ (and not simply x_1), we consider the following definition for the acoustic continuum functions

$$\frac{\omega A_1(\omega)}{2\sqrt{B_1(\omega)}}\int_{-\infty}^{+\infty}\left(\frac{\frac{2}{\sqrt{B_1(\omega)}}}{\frac{1}{B_1(\omega)}+s_1^2}\right)e^{js_1\omega x}ds_1=\frac{\omega A_1(\omega)}{2\sqrt{B_1(\omega)}}\left(e^{-\omega\frac{(x_1)}{\sqrt{B_1(\omega)}}}\right) \tag{11}$$

where B_1 must be positive for consistency reasons. Now we consider the contribution of the poles. For each of them, at each frequency and to accurately account for its dependence along s_1, we consider the following function

$$F_{pôle}(\omega,s_1)=\frac{F_p(\omega)}{s_p(\omega)-s_1}+\frac{F_p(\omega)}{s_p(\omega)+s_1}=2\left(\frac{F_p(\omega)s_p(\omega)}{s_p^2(\omega)-s_1^2}\right) \tag{12}$$

This function possesses a known Fourier transform [6] which reads

$$\int_{-\infty}^{+\infty} F_{pôle}\left(k_1\right) e^{jk_1 x_1} ds_1 = \omega \int_{-\infty}^{+\infty} F_{pôle}\left(\omega, s_1\right) e^{js_1 \omega x_1} ds_1 = 2\omega F_p\left(\omega\right) e^{js_p\left(\omega\right)\omega\left(x_1\right)} \tag{13}$$

Combining relations (11) and (13) yields the settlement of the spatial Green's function as the sum of contributions due to the poles and to the acoustic continuum. Figure 5 shows an example of this spatial Green's function, which shows on one hand the contribution of the bulk wave very closely to the point of emission and of the guided modes which of course extends at infinity as no source of losses was considered in our development. These results are in line with our understanding of the acoustical behavior of the studied structure.

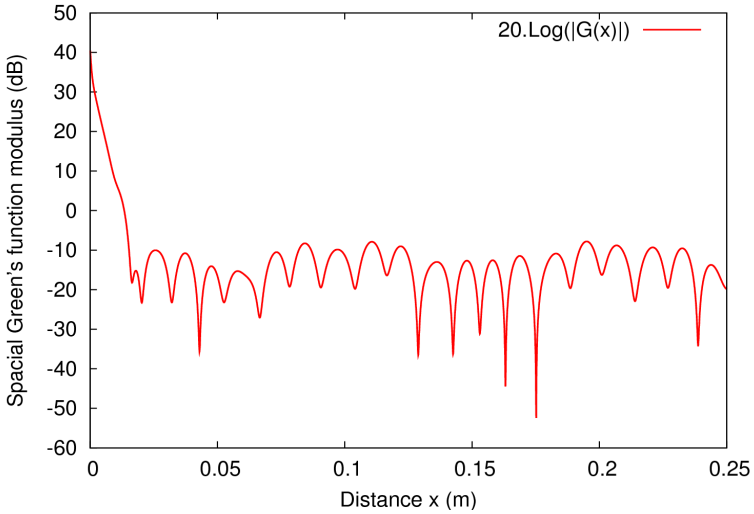

Fig.5 Spatial Green's function obtained by suming the contribution of poles and acoustic continuum at a frequency near 50 MHz

BOUNDARY INTEGRAL METHOD FOR THE SIMULATION OF ACTUAL DEVICES

We can now establish the electrical surface convolution as follows

$$\varphi\left(+e, x_1\right) = \omega \int_{-\infty}^{+\infty} g\left(\omega, \left(x_1 - x_1'\right)\right) D_2\left(+e, x_1'\right) dx_1' \text{ with } g\left(\omega, x_1\right) = F^{-1}\left(G_{44}^{tt} - \frac{G_{44}^{dt}}{G_{44}^{dd}} G_{44}^{td}\right)\left(\omega, x_1\right) \tag{14}$$

For each electrode, we assume the following description of the charge distribution using Chebyshev polynomials $T_n(x_1)$ for which the generator function correspond to the charge distribution considered here

$$D_2\left(x_1\right) = \frac{\sum_{n=0}^{N} T_n\left(\bar{x}_1\right) C_n^{(D,E)}}{\sqrt{\left(1-\bar{x}_1^2\right)}} \quad \text{where} \quad \bar{x}_1 = 2\left(\frac{x_1 - x_{c,E}}{a_E}\right) \tag{15}$$

with $C_n^{(D,E)}$ the weight of the Chebyshev development for the E^{th} electrode. A similar development is applied for computing the potential φ under the electrode E, which is iso-potential by definition. Projecting $\varphi^{(E)}$ on Chebyshev polynomial base yields

$$\varphi^{(E)}\left(x_1\right) = \sum_{n=0}^{N} T_n\left(\bar{x}_1\right) C_n^{(\varphi,E)} \quad \text{with} \quad C_n^{(\varphi,E)} = \frac{a_E \chi_n}{\pi 2} \int_{-1}^{+1} \frac{T_n\left(\bar{x}_1\right) \varphi\left(\bar{x}_1\right)}{\sqrt{1-\bar{x}_1^2}} d\bar{x}_1 \tag{16}$$

Combining (16) and (15) with (14) allows for establishing a linear algebraic system relating weights $C_n^{(D,E)}$ and $C_n^{(\varphi,E)}$ together, allowing for solving numerically the continuous problem (14), which reads

$$C_n^{(\varphi,\in)} = \sum_{E=1}^{N_E} \sum_{m=0}^{N} H_{n,m}^{(\in,E)} C_m^{(D,E)} \tag{17}$$

with $H_{n,m}^{(\in,E)} = \omega \frac{a_\in a_E \chi_n}{4\pi} \int_{-1}^{+1}\int_{-1}^{+1} \frac{T_n(\bar{x}_1)}{\sqrt{1-\bar{x}_1^2}} g\left(\omega, (a_\in \frac{\bar{x}_1}{2} + x_{c,\in} - a_E \frac{\bar{x}_1'}{2} - x_{c,E})\right) \frac{T_m(\bar{x}_1')}{\sqrt{(1-\bar{x}_1'^2)}} d\bar{x}_1' d\bar{x}_1$.

The above integrals can advantageously be performed using a Gauss-Chebyshev numerical integration scheme which nicely fit with the development we adopted, as proposed by Ribbe for SAW on semi-infinite substrates [10]. Once this system establish, the number of unknown variable must be reduced considering boundary conditions. The nature of these boundary conditions is now detailed :

i) Forced potential: the potential is forced to an harmonic value V yielding

$$V = \sum_{n=0}^{N} T_n(\bar{x}_1) C_n^{(\varphi,E)} \quad \text{with} \quad C_n^{(\varphi,E)} = V \quad \text{if} \quad n=0, \quad 0 \quad \text{otherwise since} \quad T_0(x) = 1 \tag{18}$$

ii) Free potential (zero charge) or isolated electrode: this correspond to annul the global charge under the electrode, yielding

$$\int_{-1}^{1} D_2(x_1) dx_1 = \sum_{n=0}^{N} C_n^{(D,E)} \int_{-1}^{1} \frac{T_n(\bar{x}_1)}{\sqrt{(1-\bar{x}_1^2)}} d\bar{x}_1 = 0 \;\Rightarrow\; C_0^{(D,E)} = 0 \tag{19}$$

as the integral of T_n under the electrode is zero for $n \neq 0$. $C_0^{(\varphi,E)}$ then becomes the actual unknown of the problem, the other coefficients vanishing to respect the iso-potential condition.

iii) Forced impedance: we add a supplementary relation between charge and potential $V=ZI=Z.(j\omega Q)$, with Q the total charge under the electrode

$$\int_{-1}^{1} D_2(x_1) dx_1 = C_0^{(D,E)} = \frac{V}{j\omega Z} \quad \text{considering} \quad C_0^{(\varphi,E)} = V, \quad C_{n\neq 0}^{(\varphi,E)} = 0 \tag{20}$$

We then reduce the number of unknowns by substituting $C_0^{(\varphi,E)}$ by its charge dependent expression $C_0^{(D,E)}$. Z can be complex of course and frequency dependent. This condition is of particular importance as we specifically focus on transducers loaded by a 50Ω impedance as for most of our characterizations.

SYSTEM RESOLUTION – NUMERICAL APPLICATION

The final system accounts for the boundary conditions applied on each electrodes and hence exhibits as much unknowns as equations. The H matrix in (17) is full and may need some conditioning. Whatever, for a unit potential excitation, the admittance is directly accessed by the first weight of the Chebyshev expansion of the charge times angular frequency times the electrode width (aperture) a as follows

$$Y(\omega) = j\omega Q_{tot} = j\omega\pi a C_0^{(D,E)} \tag{21}$$

As a first test, we have consider the simple case of a single top electrode atop the same AT cut quartz plate considered all along the paper, the aperture being fixed to a unit value, allowing for easily debugging the corresponding computer code. The admittance then is computed along the presented process, yielding the curve reported in fig.6. One can see that in conformity with the computation assumption the resonances of the fundamental mode and its third harmonic are found as expected. The conductance remains close to zero as no source of losses was accounted for. It is clear that this very simple case is not representative of the interest of the method but it allows for validating the approach which now can be applied trustfully for addressing more complicated electrode configuration.

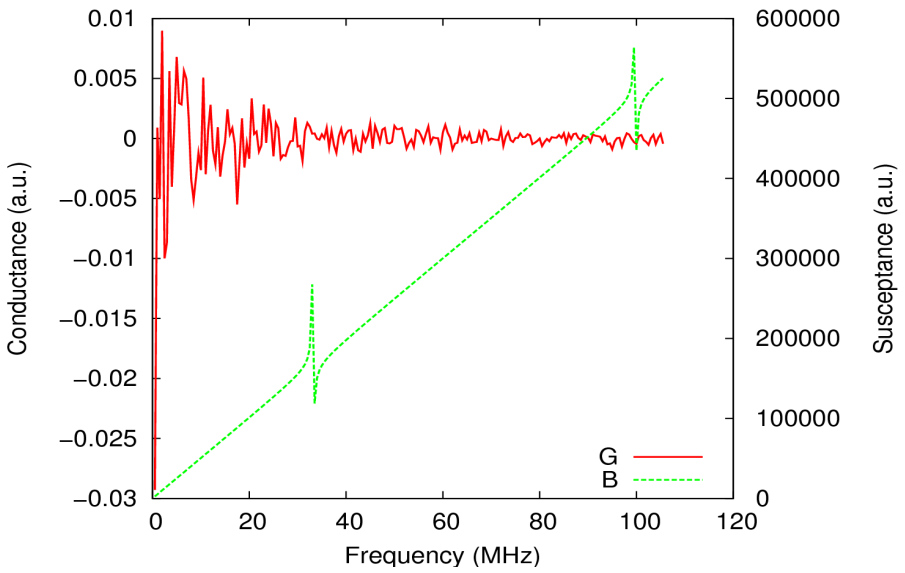

Fig.6 Example of admittance computation for a unit aperture BAW resonator on a 50µm thick AT cut quartz plate

CONCLUSION

We have presented a model dedicated to the simulation of acoustic devices built on laminar plates. The important aspect of this model is that it is based on the computation of a spatial Green's function which can be completely derived as spectral variables (slowness and angular frequency) are always separated and its singular behavior always integrable. Once this function obtained, we have shown how to simulate finite length electrode excitation of b ulk waves. Computation delays may be large when computing the spatial Green's function, but this must be done only once. The spatial Green's function then canb e interpolated, yielding notable computation gain. Consequently, a standard BAW device can be accurately simulated in a few seconds. We intend to extend this model to account for electrode mass loading and eventually to 3D problems

REFERENCES

[1] A. Reinhardt, V. Laude, A. Khelif, S. Ballandras, "Dyadic Green's functions of a laminar plate", IEEE Trans Ultrason Ferroelectr Freq Control. 2004 Sep;51(9):1157-64

[2] K.Y. Hashimoto, "Surface Acoustic Wave Devices in Telecommunications: Modelling and Simulation", Springer Verlag, 2000

[3] W.P. Mason, Physical Acoustics and the Properties of Solids, D. Van Nostrand Co., Princeton, NJ, 1958

[4] T. Makkonen, A. Holappa, J. Ella, and M. M. Salomaa, Finite Element Simulations of Thin Film Composite BAW Resonators, IEEE UFFC, Vol. 48 , Issue 5, September 2001, pp. 1241-1258

[5] D. Royer, E. Dieulesaint, « Acoustique dans les solides », Tome I, Masson Ed., 1997 – D. Royer, E. Dieulesaint, "Elastic waves in solids", Springer-Verlag Ed., 2000

[6] J.M. Hodé, J. Desbois, "Original basic properties of the Green's functions of a semi-infinite piezoelectric substrate", Proc. of the IEEE Ultrasonics Symposium, pp. 131-136, 1999

[7] P. Ventura, J.-M. Hodé, J. Desbois, M. Solal, Combined FEM and green's function analysis of periodic SAW structure, application to the calculation of reflection and scattering parameters; IEEE transactions on Ultrasonics, Ferroelectrics, and Frequency Control, vol. 48, n 5, pp. 1259-1274, 2001

[8] Erdélyi, Arthur, ed. (1954), *Tables of Integral Transforms*, **1**, New Your: McGraw-Hill

[9] A. Angot, Complément de Mathématiques, 6ème Edition, Masson Ed., 1982

[10] J. Ribbe, "On the coupling of Integral equations and finite elements/ Fourier modes for the simulation of piezoelectric surface acoustic wave components", Thèse de Doctorat de L'Ecole Polytechnique en Analyse Numérique, EP Palaiseau – X, 2000